

# Evaluating performance of neural codes in neural communication networks

Chris G. Antonopoulos<sup>1</sup>, Ezequiel B. Martinez<sup>2</sup> and Murilo S. Baptista<sup>3</sup>

August 7, 2018

<sup>1</sup>Department of Mathematical Sciences, University of Essex, Wivenhoe Park, UK

<sup>2</sup>Data Science Studio - IBM Netherlands, Amsterdam, The Netherlands

<sup>3</sup>Department of Physics (ICSMB), University of Aberdeen, SUPA, Aberdeen, UK

## Abstract

Information needs to be appropriately encoded to be reliably transmitted over a physical media. Similarly, neurons have their own codes to convey information in the brain. Even though it is well-known that neurons exchange information using a pool of several protocols of spatial-temporal encodings, the suitability of each code and their performance as a function of the network parameters and external stimuli is still one of the great mysteries in Neuroscience. This paper sheds light into this problem considering small networks of chemically and electrically coupled Hindmarsh-Rose spiking neurons. We focus on the mathematical fundamental aspects of a class of temporal and firing-rate codes that result from the neurons' action-potentials and phases, and quantify their performance by measuring the Mutual Information Rate, aka the rate of information exchange. A particularly interesting result regards the performance of the codes with respect to the way neurons are connected. We show that pairs of neurons that have the largest rate of information exchange using the interspike interval and firing-rate codes are not adjacent in the network, whereas the spiking-time and phase codes promote large exchange of information rate from adjacent neurons. This result, if possible to extend to larger neural networks, would suggest that small microcircuits of fully connected neurons, also known as cliques, would preferably exchange information using temporal codes (spiking-time and phase codes), whereas on the macroscopic scale, where typically there will be pairs of neurons that are not directly connected due to the brain's sparsity, the most efficient codes would be the firing rate and interspike interval codes, with the latter being closely related to the firing rate code.

## 1 Introduction

The main function of the brain is to process and represent information, and mediate decisions, behaviors and cognitive functions. The cerebral cortex is responsible for internal representations, maintained and used in decision making, memory, motor control, perception, and subjective experience. Recent studies have shown that the adult human brain has about  $86 \times 10^9$  neurons [13], which are connected to other neurons via as many as  $10^{15}$  synaptic connections. Neurophysiology has shown that single neurons make small and understandable contributions to behavior [24]. However, most behaviors involve large numbers of neurons, which are often organized into brain regions, with nearby neurons having similar response properties, and are spread over a number of anatomically different structures, such as the brain-stem, cerebellum, and cortex. Within each of these regions, there are different types of neurons with different connectivity-patterns and typical responses to inputs.

The coexistence of segregation and integration in the brain is the origin of neural complexity [27]. Connectivity is essential for integrating the actions of individual neurons and for enabling cognitive processes, such as memory, attention, and perception. Neurons form a network of connections and communicate with each other mainly by transmitting action potentials, or spikes. To this end, the mechanism of spike-generation is well understood: spikes generate a change in the membrane

potential of the target neuron, and when this potential surpasses some threshold, a spike (in the probabilistic sense) can be generated [17]. Brain regions show significant specialization with higher functions such as integration, abstract reasoning and consciousness all emerging from interactions across distributed functional networks of neurons in the brain.

At the local level, the workings of individual neurons is relatively well understood. However, the full understanding of the information processing in networks of spiking neurons is still elusive, i.e. the so-called “neural code”. A neural code is a system of rules and mechanisms by which a signal carries information, with coding involving various brain structures. It is clear that neurons do not communicate just by the frequency of their spikes (by a rate code) [12], as part of the information can also be transmitted in the precise timing of individual spikes [9]. These findings are still quite controversial, and whether the precise timing of spikes is important for neuronal information processing is still debatable as also is the crucial question of whether temporal structure and oscillations are relevant within the spike trains of single neurons [8]. Interactions at different timescales might be related to different types of processing, and thus, understanding information processing requires examining the temporal dynamics among neurons and in their networks. Precise spiking-time would allow neurons to communicate more information than with random spikes. However, keeping aside the question whether there is precise spiking, ideas on how such precisely timed spikes can be used are diverse as well. Different types of neural coding, including temporal and spatial coding, may also coexist on different time scales [19]. The scientific evidence collected so far supports the argument that we are still lacking a full understanding of the codes used by neurons in the brain to carry and process information.

What emerges from the scientific evidence so far suggests that fast systems and responses use fast spiking-time coding. For example, the human visual system has been shown to be capable of performing very fast classification [30], where a participating neuron can fire at most one spike! The speed involved in decoding auditory information, and even the generation of speech also suggest that most crucial neural systems of the human brain operate quite fast. For example, human fingertip sensory neurons were found to support this by demonstrating a remarkable precision in the time-to-first spikes from primary sensory neurons [16].

The debate about how information is coded and transmitted in the cortex is quite old [22] and remains highly active [28, 11, 10]. Most studies on how the brain codes information and which variables are processed within particular cortical areas make assumptions about which features of the neural responses carry information. Although most studies on sensory or motor neurophysiology assume that the spike counts of single neurons within an arbitrary time window are the relevant features of neural coding, it is still not clear. Information is also represented by spatial patterns of activity occurring over neural populations. Understanding how information is encoded in the activity of such populations is crucial for understanding the computations underlying brain functions. In vertebrates, information is often encoded by patterns of activity within neural populations responsible for similar functions. Although population representations appear to be ubiquitous in neural systems, different brain regions that perform different specific tasks, increase the difficulty of understanding the neural code. Thus, investigating the fundamental properties of neural coding in spiking neurons may allow for the interpretation of population activity and, for understanding better the limitations and abilities of neural computations.

In this paper, we study neural coding from the mathematical-modeling point of view and introduce four neural codes and their mathematical methodologies to quantify the rate of information exchanged for each code, in small networks of chemically and electrically coupled Hindmarsh-Rose (HR) spiking neurons [3, 2]. We focus on the mathematical fundamental aspects of how neurons communicate, and for this reason we do not deal with spatial codes, but only with temporal and firing-rate codes which are responsible for the exchange of information in small networks of HR neurons. For each node in the network, we record the activity in time of the action-potential variable  $p$  and its phase  $\phi$ . We then construct a suitable map representation of these variables for which we then compute the rate of information exchanged for pair-wise neurons, aka the Mutual Information Rate (MIR) [7], as a function of the way neurons are connected and of the synaptic intensities. We consider as a neural code the precise spiking-times of the neural activity (i.e. a temporal code), the maximum points of the phase of neural activities (i.e. neural phase, giving an estimation of the number of cycles of the neuron potential, considering all oscillatory behaviors with arbitrary amplitude, including the spiking high-frequency and the bursting low-frequency oscillations), the

interspike intervals (measuring only the spiking large amplitude “extreme” events), and finally the firing rate (i.e. ratio of spiking activity over a specific time interval). For the first three codes, we require that all measurements are performed with respect to the ticks of a local master “clock” [15], relative to the activity produced by one of the participating neurons in the network. The choice of the clock can be arbitrary in the sense that the activity of any single neuron in the network can be used, and that that does not alter the conclusions drawn. This is a requirement that allows for the determination of which neurons cause an effect to which other neurons in the network.

Our main findings are summarized as following: in the simplest case of a single pair of coupled spiking neurons, we find that they exchange the largest possible amount of information per unit of time when the neural code is based on the precise spiking-time. If observable noise is present in the communication, firing rates are able to exchange larger rates of information as compared to those based on temporal codes. In the case of four chemically and electrically coupled neurons, the largest rate of information exchanged can be attributed to the neural codes based on the maximum points of the phases (mod  $2\pi$ , thus a code dependent on the period of the neuron’s oscillatory behavior) and of that based on the interspike intervals. On the other hand, when neurons form a multiplex network of 20 neurons arranged in two equally-sized modules in a bottleneck configuration, communication between pair of neurons in different modules is mostly efficient when using either the spiking-time code or the maximum points of their phases. Surprisingly, pairs of neurons that exchange the largest amount of information per unit of time using the interspike interval and the firing-rate codes are not adjacent in the network, whereas the spike timing and phase codes promote large exchange of information rate from adjacent neurons in the network. The latter results provide evidence for the non-local character of firing-rate codes and the local character of precise spiking-time codes in modular dynamical networks of spiking neurons. Knowing that neurons in the brain are actually only sparsely connected, since each neuron has less than about 10000 synapses, whereas the adult human brain has on average about 86 billion neurons [13], and assuming our results can be extended to large neural networks, the interspike and firing-rate codes responsible for exchanging information between non-adjacent neurons in the neural network, should be the dominant “language” in the brain. However, knowing also that the brain has a multitude of cliques [23], i.e. small clusters of fully connected neurons, the microcircuits’ dominant neural “language” would be based on the precise spiking-time and phase codes.

## 2 Materials and Methods

### 2.1 The Hindmarsh-Rose Neural Model

We simulate the dynamics of each “neuron” by a single Hindmarsh-Rose neuron system. Namely, following Refs. [3, 2], we endow the nodes (i.e. neurons) of the networks with the dynamics characterized by [14]:

$$\begin{aligned}\dot{p} &= q - ap^3 + bp^2 - n + I_{\text{ext}}, \\ \dot{q} &= c - dp^2 - q, \\ \dot{n} &= r[s(p - p_0) - n],\end{aligned}\tag{1}$$

where  $p$  is the membrane potential,  $q$  the fast ion current, either  $Na^+$  or  $K^+$ , and  $n$  the slow ion current, for example  $Ca^{2+}$ . The parameters  $a, b, c, d$ , which model the function of the fast ion channels, and  $s, p_0$  are given by  $a = 1, b = 3, c = 1, d = 5, s = 4$  and  $p_0 = -8/5$ . The parameter  $r$ , which modulates the slow ion channels of the system, is set to 0.005, and the current that enters each neuron  $I_{\text{ext}}$  is fixed to  $I_{\text{ext}} = 3.25$ . All neurons are submitted to the same external current  $I_{\text{ext}}$  for simplicity. For these values, each neuron can exhibit chaotic behavior and the solution to  $p(t)$  exhibits typical multi-scale chaos characterized by spiking and bursting, which is consistent with the membrane potential observed in experiments made on single neurons *in vitro* [14].

We couple the HR system and create an undirected dynamical network (DN) of  $N_n$  neurons

connected by electrical (linear diffusive coupling) and chemical (nonlinear coupling) synapses:

$$\begin{aligned}
\dot{p}_i &= q_i - ap_i^3 + bp_i^2 - n_i + I_{\text{ext}} - g_n(p_i - V_{\text{syn}}) \sum_{j=1}^{N_n} \mathbf{B}_{ij} S(p_j) - g_l \sum_{j=1}^{N_n} \mathbf{G}_{ij} H(p_j), \\
\dot{q}_i &= c - dp_i^2 - q_i, \\
\dot{n}_i &= r[s(p_i - p_0) - n_i], \\
\dot{\phi}_i &= \frac{\dot{q}_i p_i - \dot{p}_i q_i}{p_i^2 + q_i^2}, \quad i = 1, \dots, N_n,
\end{aligned} \tag{2}$$

where  $\dot{\phi}_i$  is the instantaneous angular frequency of the  $i$ -th neuron [21, 20],  $\phi_i$  is the phase defined by the fast variables  $(p_i, q_i)$  of the  $i$ -th neuron,  $H(p) = p$  and  $S(p) = [1 + e^{-\lambda(p - \theta_{\text{syn}})}]^{-1}$ . The remaining parameters  $\theta_{\text{syn}} = -0.25$ ,  $\lambda = 10$ , and  $V_{\text{syn}} = 2$  are chosen so as to yield an excitatory DN. The parameters  $g_n$  and  $g_l$  denote the coupling strength associated with the chemical and electrical synapses, respectively. The chemical coupling is nonlinear and its functionality is described by the sigmoidal function  $S(p)$ , which acts as a continuous mechanism for the activation and deactivation of the chemical synapses. For the chosen parameters, we have  $|p_i| < 2$ , and  $(p_i - V_{\text{syn}})$  is always negative for excitatory networks. If two neurons are connected via an excitatory synapse, then if the presynaptic neuron spikes, it induces the postsynaptic neuron to spike. We adopt only excitatory chemical synapses in our analysis.  $\mathbf{G}_{ij}$  accounts for the way neurons are electrically (diffusively) coupled and is represented by a Laplacian matrix

$$\mathbf{G}_{ij} = \mathbf{K}_{ij} - \mathbf{A}_{ij}, \tag{3}$$

where  $\mathbf{A}$  is the binary adjacency matrix of the electrical connections and  $\mathbf{K}$  is the degree identity matrix based on  $\mathbf{A}$ , leading thus to  $\sum_{j=1}^{N_n} \mathbf{G}_{ij} = 0$ . By binary we mean that if there is a connection between two neurons, then the entry of the matrix is 1, otherwise it is 0.  $\mathbf{B}_{ij}$  is a binary adjacency matrix and describes how neurons are chemically connected and, therefore, its diagonal elements are equal to 0, thus  $\sum_{j=1}^{N_n} \mathbf{B}_{ij} = k_i$ , where  $k_i$  is the degree of the  $i$ -th neuron.  $k_i$  represents the number of chemical links that neuron  $i$  receives from all other  $j$  neurons in the network. A positive off-diagonal value of both matrices in row  $i$  and column  $j$  means that neuron  $i$  perturbs neuron  $j$  with an intensity given by  $g_l \mathbf{G}_{ij}$  (electrical diffusive coupling) or by  $g_n \mathbf{B}_{ij}$  (chemical excitatory coupling). Therefore, the adjacency matrices  $\mathbf{C}$  of the DNs are given by

$$\mathbf{C} = \mathbf{A} + \mathbf{B}. \tag{4}$$

For each neuron  $i$ , we use the following initial conditions:  $p_i = -1.30784489 + \eta_i^r$ ,  $q_i = -7.32183132 + \eta_i^r$ ,  $n_i = 3.35299859 + \eta_i^r$  and  $\phi_i = 0$ , where  $\eta_i^r$  is a uniformly distributed random number in  $[0, 0.5]$  for all  $i = 1, \dots, N_n$  (see Ref. [2] for details). These initial conditions place the trajectory quickly on the attractor of the dynamics, eliminating thus the need for time-consuming calculations.

## 2.2 Numerical Simulations and Upper Bound for MIR

We have numerically integrated Eqs. (2) using Euler's first order method with time-step  $\delta t = 0.01$  to reduce the numerical complexity and CPU time to feasible levels as a preliminary comparison for trajectories computed for the same parameters (i.e.  $\delta t$ , initial conditions, etc.) using integration methods of order 2, 3 and 4 (e.g. the Runge-Kutta method) produced similar results. The numerical integration of the HR system of Eqs. (2) was performed for a total integration time of  $t_f = 10^7$  units and the computation of the various quantities needed in our analysis were computed after a transient time  $t_t = 300$  to make sure that orbits have converged to an attractor of the dynamics.

After Shannon's pioneering work [26] on information, it became clear that it is a very useful and important concept as it can measure the amount of uncertainty an observer has about a random event and thus provides a measure of how unpredictable it is. Another concept related to Shannon entropy that can characterize random complex systems is Mutual Information (MI) [26], a measure of how much uncertainty one has about a state variable after observing another state variable in the system. In Ref. [4], the authors have derived an upper bound for the MIR between two nodes or two groups of nodes of a complex dynamical network that depends on the two largest Lyapunov

exponents  $l_1$  and  $l_2$  of the subspace of the network formed by these nodes. Particularly, they have shown that:

$$\text{MIR} \leq I_c = l_1 - l_2, \quad l_1 \geq l_2, \quad (5)$$

where  $l_1, l_2$  are the two finite-time and -size Lyapunov exponents calculated in the bi-dimensional observation space of the two considered nodes [4, 1], which typically should approach the two largest Lyapunov exponents  $\lambda_1, \lambda_2$  of the dynamics if the network is connected and the time to calculate  $l_1, l_2$  is sufficiently small. We have used the well-known method of Ref. [5] to compute the Lyapunov exponents  $\lambda_1, \lambda_2$  needed for the estimation of the upper bound  $I_c$  for MIR. In our study, the upper bound  $I_c$  for the MIR is effectively estimated by  $I_c = \lambda_1 - \lambda_2$  (i.e.  $l_1 = \lambda_1$  and  $l_2 = \lambda_2$ ) and will stand for the upper bound for the information transferred per unit of time in the DN (i.e. among the neurons). The phase spaces of the dynamical systems associated to the DNs are multi-dimensional and thus, estimating an upper bound for the MIR using  $\lambda_1$  and  $\lambda_2$  calculated by the method of Ref. [4] instead of the MIR itself, reduces considerably the complexity of the numerical calculations. Besides, parameter changes that cause positive or negative changes in the MIR are reflected in the upper bound  $I_c$  with the same proportion [4].

## 2.3 Computation of MIR for Maps

Following [6], the MIR between a pair of time-series  $X(t)$  and  $Y(t)$  (representing a mapping of any two variables in the neural codes in the next subsections), was estimated by considering binary symbolic dynamics that encode each time-series  $X(t)$  and  $Y(t)$  into the symbolic trajectory represented by  $(\alpha, \beta)$ .  $N$  sequentially mapped points of  $X(t)$  and  $Y(t)$  are encoded into the symbolic sequences  $\alpha = \alpha_1, \alpha_2, \alpha_3, \dots, \alpha_N$  and  $\beta = \beta_1, \beta_2, \beta_3, \dots, \beta_N$ , each composed by  $N$  elements. The encoding is done by firstly normalising the time-series  $X(t)$  and  $Y(t)$  to fit the unit interval  $[0, 1]$ . Both  $\alpha_i$  and  $\beta_i$  can assume only 2 values, either “0”, if the time-series value is smaller than 0.5, or “1”, otherwise.

The Mutual Information,  $\text{MI}(L)$ , between  $X(t)$  and  $Y(t)$  is thus estimated by measuring the MI between the two symbolic sequences  $\alpha$  and  $\beta$  by

$$\text{MI}_{XY}(L) = \sum_k \sum_l P(X(L)_k^\alpha, Y(L)_l^\beta) \log \frac{P(X(L)_k^\alpha, Y(L)_l^\beta)}{P(X(L)_k^\alpha)P(Y(L)_l^\beta)}, \quad (6)$$

where  $P(X(L)_k^\alpha, Y(L)_l^\beta)$  is the joint probability between symbolic sequences of length  $L$  observed simultaneously in  $\alpha$  and  $\beta$ , and  $P(X(L)_k^\alpha)$  and  $P(Y(L)_l^\beta)$  are the marginal probabilities of symbolic sequences of length  $L$  in the sequences  $\alpha$  and  $\beta$ , respectively. The subindices  $k$  and  $l$  vary from 1 up to the number of symbolic sequences of different lengths  $L$  observed in  $\alpha$  and  $\beta$ , respectively.

MIR is then estimated by the slope of the curve of the MI for symbolic sequences of length  $L \in [2, 5]$  with respect to  $L$ , which is an estimation of the increase of MI per time interval. More details can be found in [6].

## 2.4 Neural Codes

Below, we introduce four neural codes and their corresponding methodologies to quantify the rate of information exchanged between pairs of neurons.

The first uses the spiking-times of neural activity (temporal code), the second the maximum points of the phase of neural activities (neural phase), the third the interspike intervals and the last, the firing rates (ratio of spiking activity over a specific time interval). The first three require that all recordings are done with respect to the ticks of a local master “clock” [15], relative to the activity produced by a single neuron. The choice of the clock can be arbitrary in the sense that the activity of any single neuron can serve as the clock, and that that does not alter the final conclusions drawn whatsoever.

### 2.4.1 Neural Code Based on spiking-times: $\text{MIR}_{st}$

Here, we describe how we compute the amount of information exchanged per unit of time between neurons  $i, j$  based on the spiking-times of the first neuron,  $\text{MIR}_{st}$ . Particularly, we assume that

the first neuron plays the role of the clock and record in time the  $p$  values from Eq. (2) of both neurons  $i, j$  at times when the  $p$  variable of the first neuron attains its local maxima. This allows us to construct a time-series of spike events  $X_i, Y_j$  by transforming the continuous dynamics of the  $p$  variables of both neurons  $i, j$  into a time-series of discrete-time spike events. We then use the time-series  $X_i, Y_j$  to compute the rate of information exchanged between neurons  $i$  and  $j$  as explained in Subsec. 2.3. We divide the rate of information exchanged by the mean of the interspike times of the spike activity of the first neuron (i.e. the “clock”). We call this quantity the  $\text{MIR}_{st}$  of pair of neurons  $i, j$ .

#### 2.4.2 Neural Code Based on the Phase: $\text{MIR}_{m\phi}$

Next, we explain how we compute the amount of information exchanged per unit of time between two neurons  $i, j$  based on the maximum points of the time evolution of the phase variable  $\phi$ , what we denote by  $\text{MIR}_{m\phi}$ . We assume again that the first neuron plays the role of the “clock” and record in time  $\Phi \equiv \text{mod}(\phi, 2\pi)$  from Eq. (2) of both neurons  $i, j$  at times when  $\Phi$  of the first neuron attains local maxima. This allows us to construct a time-series of events  $X_i, Y_j$  by transforming the continuous dynamics of the phase variables of both neurons into a time-series of discrete time events. We then use  $X_i, Y_j$  to compute the rate of information exchanged between neurons  $i, j$ . We divide the rate of information exchanged by the mean of the time intervals for  $\Phi$  of the first neuron (i.e. the “clock”) to attain its local maxima. We call this quantity the  $\text{MIR}_{m\phi}$  of pair  $i, j$ .

#### 2.4.3 Neural Code Based on the Interspike Intervals: $\text{MIR}_{ii}$

Here we discuss about the computation of the amount of information exchanged per unit of time between two neurons  $i, j$  based on the interspike intervals of their  $p$  variables, denoted by  $\text{MIR}_{ii}$ . Similarly, we assume that neuron  $i$  plays the role of the “clock” and record in time the interspike intervals of both neurons  $i, j$  whenever the spike of neuron  $j$  occurs after that of neuron  $i$ . This allows us to construct a time-series of interspike events  $X_i, Y_j$  from the continuous trajectories of both neurons. We then use  $X_i, Y_j$  to compute the rate of information exchanged between neurons  $i$  and  $j$ , dividing this amount by the mean of the time intervals constructed as the difference between the spiking-times of neuron  $j$  and those of neuron  $i$ , given that the spike of neuron  $j$  occurred after that of neuron  $i$ . We call this quantity the  $\text{MIR}_{ii}$  of pair  $i, j$ , where the subscript  $ii$  stands for interspike intervals.

#### 2.4.4 Neural Code Based on the Firing Rates: $\text{MIR}_{fr}$

Finally, we show how we compute the amount of information exchanged per unit of time between neurons  $i, j$  based on the firing rates of their  $p$  variables,  $\text{MIR}_{fr}$ . Here, we divide the time window between the first and last recorded spiking-time of neuron  $i$  into  $1.5 \times 10^6$  equally sized time windows, and compute the firing rates for both neurons in these time windows. By firing rate, we mean the ratio between the number of spikes in a given time interval divided by the length of the time interval. This allows us to construct a time-series of firing rate events  $X_i, Y_j$ . We then use these time-series to compute the rate of information exchanged between neurons  $i, j$ , dividing it by the length of the equally-sized time windows. We call this quantity the  $\text{MIR}_{fr}$  of pair  $i, j$ .

## 3 Results

### 3.1 Neural Codes for the Communication of Two Neurons

We study the four neural codes introduced in Subsec. 2.4, in the simplest case of a pair of chemically and bidirectionally connected HR neurons (see Fig. 1a)), in the absence of noise. We consider the effect of noise in the performance of the neural codes in the next section. Our goal is to understand which neural code can maximize the rate of information-exchange between the two neurons, considering them as a communication system and for which chemical coupling strengths  $g_n$  this happens. We note that we are not interested in the directionality of the information flow

but only on the rate of information exchanged pair-wise. Particularly, in Fig. 1 we calculate the amount of MI per unit of time exchanged between the two neurons, *aka* their MIR, for different chemical coupling strengths  $g_n$ , for the four neural codes.

We first see in Fig. 1b) that  $MIR_{st}$  and  $MIR_{m\phi}$  are bigger than  $MIR_{ii}$  and  $MIR_{fr}$  in certain regions of intermediate and large enough chemical coupling strengths  $g_n$ . However, almost all MIR quantities are smaller than the upper bound for MIR,  $I_c$ , for five chemical coupling strengths, ranging from small to large values. We note that for  $g_n$  values larger than about 1.3, the dynamics becomes quasi-periodic and thus, there is no production of information.

In Fig. 1b), we present the MIR based on the spiking-times of both neurons ( $MIR_{st}$ ), the MIR for the maximum values of the phase ( $MIR_{m\phi}$ ), the MIR of the interspike intervals ( $MIR_{ii}$ ) and the MIR of the firing rates ( $MIR_{fr}$ ). We also plot the upper bound for MIR, i.e.  $I_c = \lambda_1 - \lambda_2$ , an upper bound for MIR [4]. We focus on three characteristic cases: the first corresponds to the case where  $MIR_{m\phi} > MIR_{st}$  for chemical coupling strength  $g_n = 0.1$ . The second, to a case where  $MIR_{ii} > I_c$ ,  $MIR_{m\phi}$  and  $MIR_{st}$  for  $g_n = 0.48$  (one of the five distinct cases where the computed MIR is bigger than the upper bound  $I_c$ ), and the last one to a case where  $MIR_{st} > MIR_{m\phi}$  for  $g_n = 1$ . In the first case, the two neurons communicate more efficiently by exchanging larger amounts of information per unit of time using their phases whereas the third one to the case where they communicate more efficiently by exchanging information by the precise spiking-times. In the second case, the two neurons communicate more efficiently by encoding their information in their interspike activity.

To appreciate the performance of the different neural codes used by the two neurons for optimal communication, we first focus on the case of  $g_n = 0.1$  for which  $MIR_{m\phi} > MIR_{st}$ , and plot in panel c) of Fig. 1, the time evolution of  $p$  variables of both neurons, the data used to compute  $MIR_{st}$  in panel d), the plane of the phase variables of both neurons ( $\Phi_1, \Phi_2$ ) in panel e), in which the computation of  $MIR_{m\phi}$  is based, and in panel f) the data used to compute  $MIR_{ii}$ , where  $\tau_i$ ,  $i = 1, 2$  are the interspike intervals of both neurons. We observe in panel c) that the spike times of both neurons are different and particularly, from panel d) one realizes that when the first neuron spikes, the second usually does not spike as there is a high density of  $p_2$  values around -1, with spikes occurring around  $p_2 \approx 1.9$ . This behavior is due to the second neuron which is actually in its quiescent period when the first is spiking. In contrast, when observing the plane of phases in panel e), it becomes apparent that there are two regions of high phase-synchronicity (i.e. stripes of high concentration) and the rest of the region with considerably smaller concentration of phase points. This behavior indicates that the two neurons communicate in time by chaotically adapting their phase activity. For the same  $g_n$ , panel f) indicates that the interspike activity of both neurons is well spread in the plane with a high concentration of points occurring close to the origin. Moreover,  $MIR_{fr}$  is seen to attain the smaller value with respect to all other quantities considered in this work. These results justify why  $MIR_{m\phi} > MIR_{st}$  for this coupling strength.

In panels g) to j) we study the second case, for  $g_n = 0.48$ , for which  $MIR_{ii} > I_c$ . We remark however that this apparent violation comes about because we estimate  $I_c$  by the Lyapunov exponents and not by the expansion rates. Since MIR is estimated by a mesh grid of finite resolution, an upper bound for MIR calculated for this grid would require the calculation of expansion rates using the very same grid resolution.  $I_c$  estimated by Lyapunov exponents is smaller than the bound estimated by expansion rates (see Supplementary material in [4]). Therefore,  $I_c$  in this case could not be a true upper bound for MIR and we want to understand why this is so. Here, we also observe that  $MIR_{st} > MIR_{m\phi}$  (see panel b)), a result that indicates that the two neurons communicate mostly by exchanging information by their precise spiking-times and less by their phases. This can be appreciated in panel g) where both  $p$  variables attain approximately similar amplitudes during their time evolution and, becomes evident in panel h) where the second neuron spikes when the first neuron spikes and that both attain approximately the same amplitudes in their  $p$  time evolution. This behavior is highly localized. In contrast, panel i) shows that their phases actually spread all over the  $[0, 2\pi] \times [0, 2\pi]$  region and that there is no localization of points as it happened in the case of  $g_n = 0.1$  in which the two neurons communicate by exchanging the largest amount of information per unit of time by their phases. Here, panel j) indicates that the interspike activity of both neurons is well localized in two regions with high concentration closer to the origin and on the right upper part of the plot. Moreover,  $MIR_{fr}$  is seen to attain the smaller value with respect to all other quantities for this particular chemical coupling strength. These

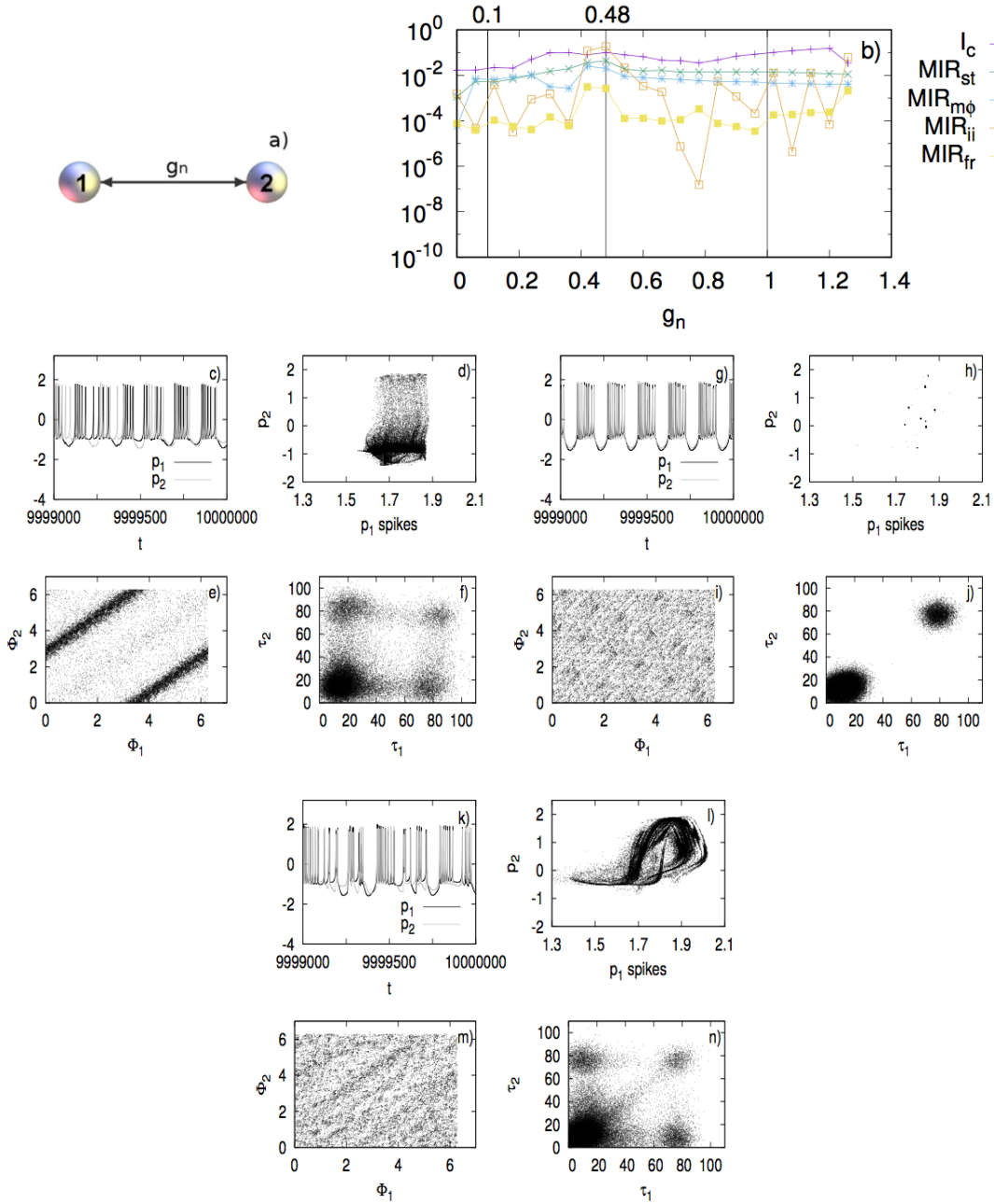


Figure 1: **Results for the neural communication channel and the code used between two chemically, bidirectionally, connected non-noisy HR neurons.** Panel a) The pair of chemically connected neurons, where  $g_n$  is the strength of the chemical coupling. Panel b)  $I_c$ , the MIR of spiking-times  $MIR_{st}$ , MIR of the maxima of the phases  $MIR_{m\phi}$ , MIR of the interspike intervals  $MIR_{ii}$  and MIR of the firing rates  $MIR_{fr}$ , respectively. Panels c) to f)  $p_1, p_2$  as a function of time (c)), the plane of phase variables  $(\Phi_1, \Phi_2)$  (d) and, the data used to compute  $MIR_{ii}$  (f)), where  $\tau_i$ ,  $i = 1, 2$  are the interspike intervals of both neurons. Panels g) to j) similarly for  $g_n = 0.48$  and panels k) to n) for  $g_n = 1$ . In panel b),  $g_n = 0.1$  that corresponds to a case where  $MIR_{m\phi} > MIR_{st}$ ,  $g_n = 0.48$  to a case where  $MIR_{ii} > I_c$ ,  $MIR_{m\phi}$  and  $MIR_{st}$ , and the case for  $g_n = 1$  that corresponds to  $MIR_{st} > MIR_{m\phi}$ .

results justify why  $MIR_{st} > MIR_{m\phi}$  for  $g_n = 0.48$ .

Finally, we focus on the third characteristic case in which  $MIR_{st} > MIR_{m\phi}$  for  $g_n = 1$ . The situation here is quite different. Panel k) reveals a phenomenon in which the spike times and

quiescent periods of both neurons are actually similar. Particularly, panel l) reveals that most of the times, either when the first neuron spikes, the second spikes or when the first is in its quiescent period, so is the second, showing a higher density of points in the upper right corner of the plot (spike activity) and a smaller one in its lower left corner (quiescent period). In contrast, the plane of phases in panel m) reveals there is no phase synchronization in their activity, as there are no regions of high concentration as in the first case in which  $MIR_{m\phi} > MIR_{st}$ . These results show that the two neurons communicate by their spiking-times, i.e. they use a temporal neural code in which the time of each spike conveys information that is transmitted to other neurons. Lastly, panel n) exhibits an interspike activity mostly concentrated in the lower left corner of the plot and less in the other three, a situation completely different to the behavior in panel j) of the second case.  $MIR_{fr}$  is seen here to attain the smaller value with respect to the other quantities, similarly to the first case. These results justify why  $MIR_{m\phi} > MIR_{st}$  for such coupling strengths.

### 3.2 Neural Codes for the Communication Between Two Noisy Neurons

We now study the same problem discussed in the previous section, in the presence of noise. We consider the effect of additive Gaussian white noise in the performance of the neural codes introduced in Subsec. 2.4. Our goal is to understand which neural code is more robust to the increase of the noise strength  $\sigma$ , a case which is more close to realistic neural behavior [25, 29]. Particularly, in the neural activity of variable  $p$  of each neuron, we add white Gaussian noise with standard deviation  $\sigma$  to obtain its noisy signal  $\bar{p}$ :

$$\bar{p} = p + \sigma\mathcal{N}(0, 1), \quad (7)$$

where  $\mathcal{N}(0, 1)$  is the Gaussian distribution of zero mean and standard deviation equal to 1. We then use such noisy data to compute the MIR of the different neural codes for different chemical coupling strengths and noise strengths  $\sigma$ .

We plot the results of these computations in Fig. 2, in particular the MIR between the two neurons in Fig. 1a), for different chemical coupling and three noise strengths. The first panel in Fig. 2 shows the same MIR quantities of Fig. 1b) but for  $\sigma = 0.4$ , the second for  $\sigma = 0.8$  and the third one for  $\sigma = 1.5$ . As the noise strength  $\sigma$  increases from zero, all MIR quantities start decreasing, except  $MIR_{fr}$ , which remains practically unaffected by the increase of the noise strength! Figure 2 reveals also that even though for small noise strengths,  $MIR_{st}$ ,  $MIR_{m\phi}$  and  $MIR_{ii}$  are larger than  $MIR_{fr}$ , they are nevertheless considerably affected by the increase of the noise strength. On the contrary,  $MIR_{fr}$  proves to be consistently robust with respect to the increase of  $\sigma$ , even for values as high as 1.5! This result underlines the importance of firing rates against temporal neural codes, such as spiking-times or those based on the phase or interspike intervals, which all prove to be more prone to noise contamination and to the transmission of smaller amounts of information per unit of time with the increase of noise strength, leading thus to the decrease of their information content.

### 3.3 Neural Codes in a Communication System of Four Neurons

Here, we extend the previous study in the case of a model of four bidirectionally connected non-noisy HR neurons, which are chemically and electrically coupled as shown in Fig. 3a). The first neuron is electrically connected with the third, whereas the first with the second and, the third with the fourth are chemically connected. The strength of the electrical connection is given by  $g_l$  and of the chemical by  $g_n$ . We aim to understanding which neural code is best suited for the maximization of the rate of information-exchange for different coupling strengths and also, to which pairs of neurons this can be attributed to. The first and third neurons are the intermediates for the communication between the second and the fourth. We consider the setup of Fig. 3a) as a communication system in which, information is transmitted through the connections and reaches the different parts.

In the following, we study the four neural codes for the model of four non-noisy neurons in Fig. 3a). We plot in panels b) and c) the parameter spaces  $(g_n, g_l)$  for the  $MIR_{st}$  of the spiking-times and for the links that maximize the same quantity, respectively. The orange spots in panel b) correspond to couplings that produce the largest amounts of  $MIR_{st}$  whereas blue to regions with

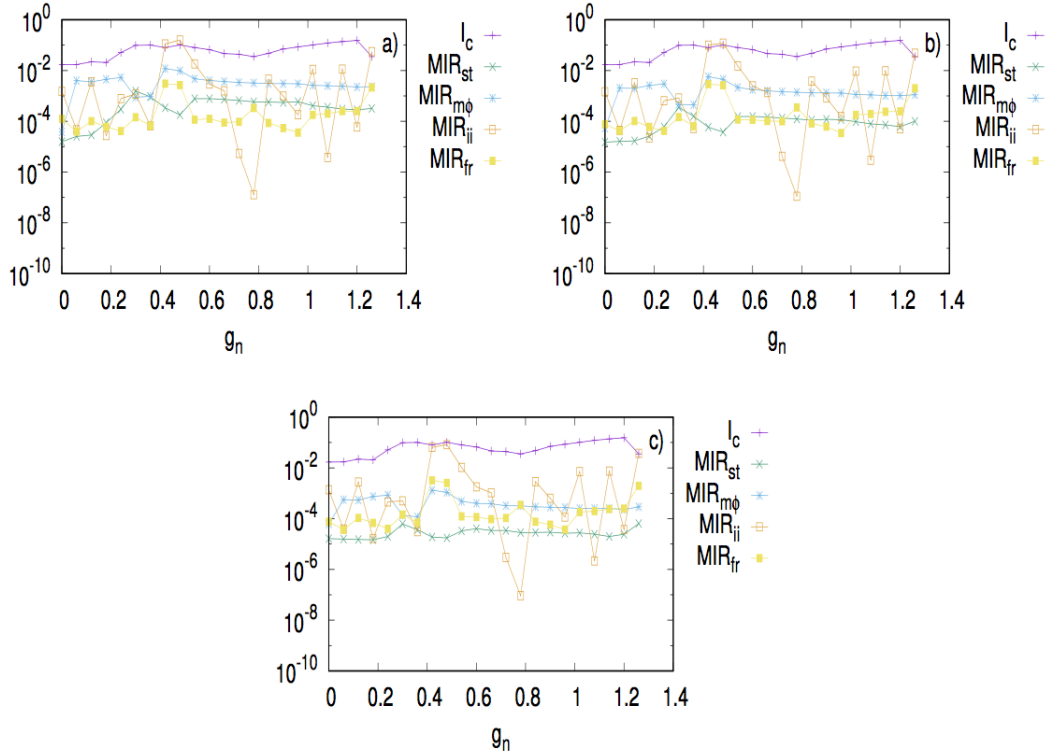


Figure 2: **Results for the neural code used among two chemically connected noisy HR neurons.** Panel a) The MIR values of the different neural codes for noise strength  $\sigma = 0.4$ . Panel b) is similar to a) but for noise strength  $\sigma = 0.8$  and panel c) for  $\sigma = 1.5$ .

the smallest  $MIR_{st}$ . The former occurs for relatively big chemical and electrical couplings whereas the latter for very small electrical and, small to large chemical couplings. Panel c) reveals that, depending on the coupling values, the largest amounts of  $MIR_{st}$  are transmitted between different pairs of neurons, giving rise to a complicated pattern in the parameter space (see Fig. 3). The pattern however is characterized by mainly the pair of neurons 3,4 (red) for small chemical and small to large electrical coupling strengths, by pair 1,2 (black) for comparatively small to large chemical and small to large electrical coupling strengths, and by many smaller-sized regions of different colours, such as blue, magenta, green and yellow that correspond to the other pairs of neurons.

The parameter space for  $MIR_{m\phi}$  in panel d) is mainly dominated by red (that corresponds to comparatively large values), a smaller blue region of moderately very low values and a smaller orange region, for high chemical and electrical couplings, that corresponds to the highest observed  $MIR_{m\phi}$  values in the parameter space. Similarly to panel c) (for  $MIR_{st}$ ), panel e) for the pairs of neurons that maximize  $MIR_{m\phi}$  shows that, depending on the coupling values, the largest amounts of  $MIR_{m\phi}$  are transmitted between different pairs of neurons, creating again a complicated pattern in the parameter space, dominated mainly by the pair of neurons 3,4 (red) for small chemical and small to large electrical coupling strengths, by pair 1,2 (black) for comparatively small to large chemical and small to large electrical coupling strengths, and by many smaller-sized regions of different colours, (i.e. blue, magenta, green and yellow) that correspond to the remaining pairs of neurons.

The situation changes slightly in panel f) for  $MIR_{ii}$  of the interspike intervals where almost all the parameter space is dominated by red (of moderately large  $MIR_{ii}$  values) with a few orange spots (very large values) and blue spots (of very low  $MIR_{ii}$  values). The blue regions are considerably smaller in size than the blue region of panel d). The case for the MIR of the interspike intervals,  $MIR_{ii}$ , is also different with respect to the pairs of neurons for which  $MIR_{ii}$  is maximal. The

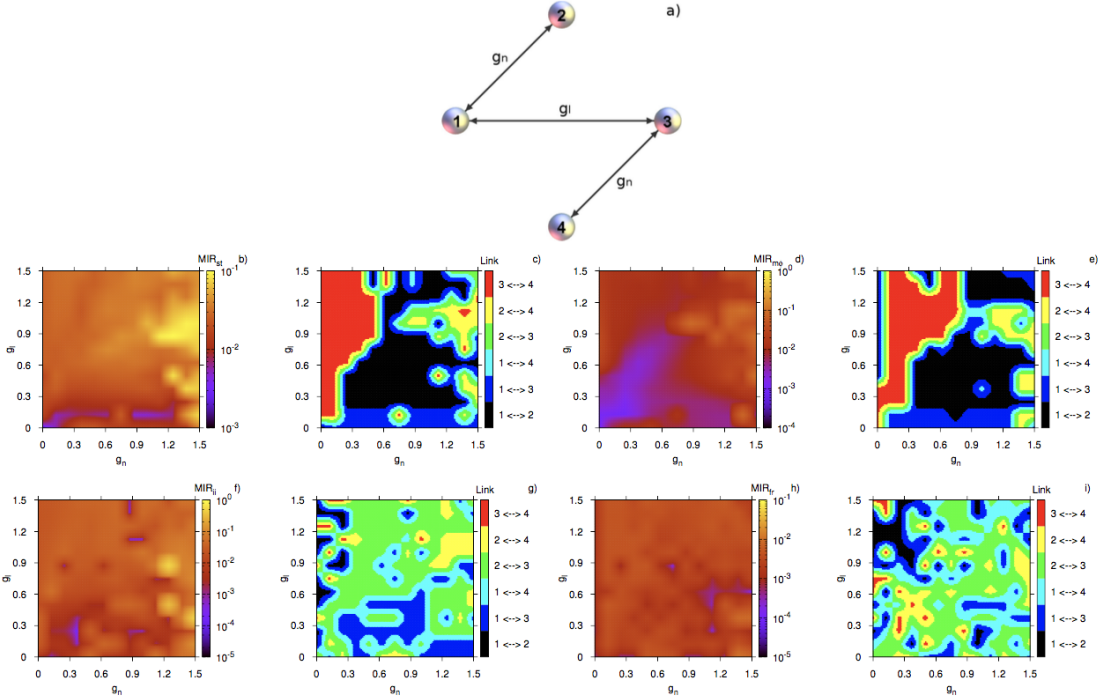


Figure 3: **Parameter spaces for the neural codes for four non-noisy HR neurons.** Panel a) The network of connections of the four neurons, where  $g_n$  is the strength of the chemical and  $g_l$  of the electrical coupling. Panels b) and c) The parameter spaces for  $MIR_{st}$  for the two nodes that provide the largest MIR value and for the links that maximize the same quantity. Panels d) and e) The parameter spaces for  $MIR_{m\phi}$  for the pair of nodes that exchange the largest amount of MIR and for the links that maximize the same quantity. Panels f) and g) The parameter spaces for  $MIR_{ii}$  between the two nodes that exchanges the largest value of MIR and for the links that maximize the same quantity. Panels h) and i) The parameter spaces for  $MIR_{fr}$  between the two nodes that exchange the largest amount of MIR and for the links that maximize the same quantity. In all cases, the notation  $i \leftrightarrow j$  in the legends indicates the bidirectional transfer of information between neurons  $i$  and  $j$ .

parameter space of panel g) reveals completely different structural properties than those of panels c) and e). Interestingly, the largest amounts of  $MIR_{ii}$  occur for all pairs except 3,4 and, less between 1 and 2, implying that the first and third neuron play mainly the role of the mediators in the transmission of information in the system.

Finally, a similar situation is happening for  $MIR_{fr}$ , with the parameter space in panel h) looking more uniformly covered by red of moderately high  $MIR_{fr}$  values and with a few quite small blue spots of very low values.  $MIR_{fr}$  seems to be much less depended on the coupling strengths though. The parameter space for the links that maximize this quantity looks quite similar to the one for  $MIR_{ii}$ , in the sense that the largest amounts of  $MIR_{fr}$  are happening for all pairs except 3,4 (red) and, less between 1 and 2 (black), implying that the first and third neuron play again the role of the mediators in the transmission of information in the system.

A comparison between the parameter spaces for the MIR quantities of Fig. 3 shows that the highest amount of information exchanged per unit of time in the system can be attributed to the neural codes of the maximum points of the phase  $MIR_{m\phi}$  and to the interspike intervals,  $MIR_{ii}$ . This is occurring for chemical coupling strengths quite big and electrical moderately smaller. Furthermore, the neural code based on the firing rates is practically unaffected by the coupling strengths, even though its maximum values are smaller than the maximum values of the neural codes based on the maximum points of the phase and interspike intervals. This result is in agreement with the performance of the same neural code in the case of the two neurons of Sec.

3.1, where it attained the lowest values of all other neural codes. Surprisingly, the pair of nodes more likely to exchange the largest amount of information per unit of time using the interspike interval and the frequency-rate codes are not adjacent in the network, whereas the spiking-time and the phase-codes promote large exchange of information from adjacent nodes in the network. This provides evidence for the non-local character of frequency-rate codes and local character of precise spiking-time codes.

### 3.4 Neural Codes in a Network of Twenty Neurons in a Bottleneck Configuration

In this section, we study the same neural codes in an extended model that comprises two identical clusters of 10 HR, non-noisy, neurons each. For simplicity, the clusters have the same small-world structure and their neurons are internally coupled with electrical connections of strength  $g_l$ . This construction is interesting as it resembles a bottleneck, in which the two clusters communicate with themselves through the only link between the first and the eleventh neuron in the two clusters. The bottleneck is represented by a single, chemical link with strength  $g_n$  that connects the two clusters. We used only one such inter-connection because this is the simplest case in which we know that information travels from one cluster to the other through the only chemical link that forms the bottleneck. Moreover, it allows us to draw interesting conclusions with regard to the neural codes adopted by the neurons for different coupling strengths. Again, the network is undirected. We present the structure of this model in Fig. 4a). Its construction is motivated by the modular organization of the brain in which neurons are linked together to perform certain tasks and cognitive functions, such as pattern recognition, function approximation, data processing, etc. Modular processors have to be sufficiently isolated and dynamically differentiated to achieve independent computations, but also globally connected to be integrated in coherent functions [31, 18]. The structure in Fig. 4a) help us understand which neural code in modular neural networks is best suited for the transmission of the largest amount of information per unit of time and for which coupling strengths this occurs. Again, we treat the model in Fig. 4a) as a communication system in which, information is transmitted through the links and reaches out to its different parts.

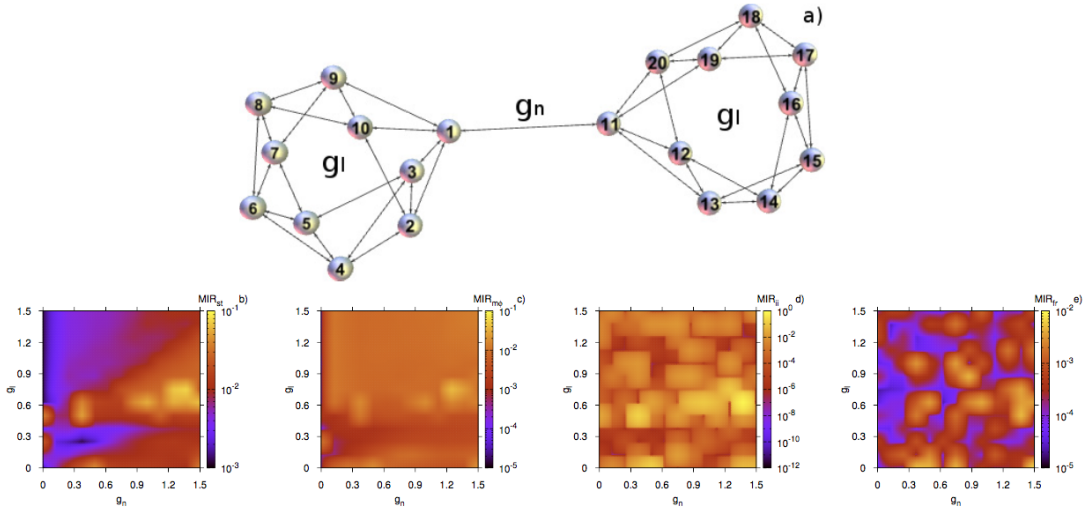


Figure 4: **Parameter spaces for the neural codes between two chemically connected non-noisy identical small-world electrically coupled clusters of 10 HR neurons each, in a bottleneck configuration.** Panel a) The two clusters of electrically connected neurons with coupling strength  $g_l$  and chemically interconnected with chemical intercluster strength  $g_n$ . Panel b) The parameter space for the MIR of spiking-times  $MIR_{st}$ , Panel c) for the MIR of the maxima of the phases  $MIR_{m\phi}$ , Panel d) for the MIR of the interspike intervals  $MIR_{ii}$  and Panel e) for the MIR of the firing rates  $MIR_{fr}$ , respectively. The colour indicates the maximal MIR value that any two nodes exchange using a particular neural code.

We study in Fig. 4 the four neural codes for the model in panel a). Panels b) and c) show the parameter space  $(g_n, g_l)$  for the  $MIR_{st}$  of the spiking-times and for the  $MIR_{m\phi}$  for the maximum points of the phase, respectively. Orange corresponds to couplings that produce the largest amounts of MIR values whereas blue or black to regions with the smallest MIR values. Red is for intermediate MIR values. Panel b) for the MIR of the spiking-times,  $MIR_{st}$ , reveals that the highest values can be achieved for large chemical and intermediate electrical coupling strengths. For example, for zero chemical coupling (i.e.  $g_n = 0$ ),  $MIR_{st}$  is considerably smaller than that of much larger  $g_n$  around 1.4. This finding underlines the importance of the chemical connections among the clusters that play the role of modular processors as they help the system transmit larger rates of information when neurons exchange information by the precise spiking-times (temporal neural code). In contrast to the behavior of  $MIR_{st}$ ,  $MIR_{m\phi}$  seems to perform more consistently in the sense that the parameter space in panel c) is more uniformly red with a few orange hot spots of large MIR values. Interestingly, this quantity becomes maximal again for large chemical and moderate electrical coupling strengths, similarly to  $MIR_{st}$ . The situation is similar for  $MIR_{ii}$ , where again it becomes maximal for large chemical and moderate electrical coupling strengths. We note that the maximum values of  $MIR_{ii}$  of the orange hot spots in panel d) are bigger by one order of magnitude than the maximum MIR values in panels b) and c). Finally, the neural code based on the firing rates,  $MIR_{fr}$ , still shows the same dependence on the coupling strengths to achieve its maximum values, even though these maximum values are smaller by one or two orders of magnitude with respect to those of the other three neural codes. Lastly, for  $MIR_{fr}$ , there are blue regions of very small values, distributed evenly in all parts of the parameter space.

Comparing the behavior of the various neural codes, we conclude that the one based on the firing rates seems to be less advantageous with respect to the maximum amounts of transmitted information per unit of time of the rest. Our results suggest that it is more prominent for neurons to use temporal codes or the maximum points of their phases to communicate the maximal rate of information in modular neural networks, for chemical coupling strengths twice as that of the electrical coupling.

## 4 Discussion

In this paper we have sought to study how information is encoded in neural activity as it is crucial for understanding the computations underlying brain functions. Information is encoded by patterns of activity within neural populations responsible for similar functions and the interest in studying them is related to how the “neural code” can be read, mainly to understand how the brain processes information to accomplish behavior and cognitive functions. Thus, investigating the fundamental properties of neural coding in networks of spiking neurons may allow for the interpretation of population activity and, for understanding better the limitations and abilities of neural computations.

In line with this, we have studied neural coding in small networks of chemically and electrically coupled Hindmarsh-Rose spiking neurons. We have introduced four such codes and their mathematical methodologies to quantify the rate of information exchange for each code. We focused on the mathematical fundamental aspects of the communication of neurons and based our study on recorded action-potentials and phases to construct suitable map-representations to compute the rate of information exchanged, quantities based on Mutual Information Rate. In the simplest case of pairs of spiking neurons we have found that they exchange the largest amount of information per unit of time by opting for a temporal code in which the time of each spike conveys information which is transmitted to the other participating neuron. However, the case is different when noise is present in the signals, in the sense that firing rates are those that can exchange large amounts of information per unit of time with respect to temporal codes. We have also studied four chemically and electrically coupled neurons and found that the largest rates of information exchange are attributed to the neural codes of maximum points of their phases and interspike intervals.

For a relatively larger network of 20 neurons arranged in two equally-sized small-world modules forming a bottleneck, our work reveals that neurons choose a temporal code or the maximum points of their phases to transmit the maximal rate of information for chemical coupling strengths twice as that of the electrical coupling. Surprisingly, pairs of nodes that are likely to exchange

the largest amount of information per unit of time using the interspike interval and frequency-rate codes are not adjacent in the network, whereas the spiking-time and phase-codes promote large exchange rate of information for adjacent neurons in the network. Our results provide evidence for the non-local character of frequency-rate codes and local character of precise spiking-time codes in modular dynamical networks of spiking neurons.

Finally, we have shown the importance of firing rates against temporal neural codes, such as spiking-times or those based on the phase or interspike intervals, which all prove to be more prone to noise contamination and to the transmission of smaller amounts of information per unit of time with the increase of noise strength, leading thus to the loss of their information content.

## Acknowledgments

This work was performed using both the Maxwell high performance computing cluster and ICSMB cluster of the University of Aberdeen. All authors acknowledge financial support provided by the EPSRC Ref: EP/I032606/1 grant. C. G. A. contributed to this work while working at the University of Aberdeen and then, when working at the University of Essex.

## References

- [1] C. G. Antonopoulos, E. Bianco-Martinez, and M. S. Baptista. Production and transfer of energy and information in Hamiltonian systems. *PLoS ONE*, 9(2):e89585, 2014.
- [2] Ch. G. Antonopoulos, S. Srivastava, E. de S. S. Pinto, and M. S. Baptista. Do brain networks evolve by maximizing their information flow capacity? *PLoS Comput. Biol.*, 11(8):e1004372, 2015.
- [3] M. S. Baptista, F. M. Kakmeni, and C. Grebogi. Combined effect of chemical and electrical synapses in Hindmarsh-Rose neural networks on synchronization and the rate of information. *Phys. Rev. E*, 82:036203, 2010.
- [4] M. S. Baptista, R. M. Rubinger, E. R. Viana, J. C. Sartorelli, U. Parlitz, and C. Grebogi. Mutual information rate and bounds for it. *PLoS One*, 7:10:e46745, 2012.
- [5] G. Benettin, L. Galgani, A. Giorgilli, and J-M. Strelcyn. Lyapunov characteristic exponents for smooth dynamical systems and for Hamiltonian systems: A method for computing all of them. Part 1: Theory and Lyapunov characteristic exponents for smooth dynamical systems and for Hamiltonian systems: A method for computing all of them. Part 2: Numerical application. *Meccanica*, 15:9–20, 21–30, 1980.
- [6] E. Bianco-Martinez and Murilo S. Baptista. Space-time nature of causality. *arXiv*, page 1612.05023, 2016.
- [7] E. Bianco-Martinez, N. Rubido, Ch. G. Antonopoulos, and M. S. Baptista. Successful network inference from time-series data using mutual information rate. *Chaos: An Interdisciplinary Journal of Nonlinear Science*, 26(4):043102, 2016.
- [8] A. Borst and F. E. Theunissen. Information theory and neural coding. *Nat. Neurosc.*, 2:947–957, 1999.
- [9] S. M. Both. The evidence for neural information processing with precise spike-times: A survey. *Natural Computing*, 3:195–206, 2004.
- [10] J. P. Gallivan and J. C. Culham. Neural coding within human brain areas involved in actions. *Current Opinion in Neurobiology*, 33:141–149, 2015.
- [11] W. Gerstner, W. M. Kistler, RR. Naud, and L. Paninski. *Neuronal Dynamics: From Single Neurons to Networks and Models of Cognition*. Cambridge University Press, 2014.

- [12] W. Gerstner, A. K. Kreiter, H. Markram, and A. V. M. Herz. Neural codes: Firing rates and beyond. *Proc. Natl. Acad. Sci. USA*, 94:12740–12741, 1997.
- [13] S. Herculano-Houzel. The remarkable, yet not extraordinary, human brain as a scaled-up primate brain and its associated cost. *Proc. Natl. Acad. Sci. USA*, 109:10661, 2012.
- [14] J. L. Hindmarsh and R. M. Rose. A model of neuronal bursting using three coupled first order differential equations. *Proc. R. Soc. London*, Ser. B 221:87–102, 1984.
- [15] J. J. Hopfield. Pattern recognition computation using action potential timing for stimulus representation. *Nature*, 376:33, 1995.
- [16] R. Johansson and I. Birznieks. Fist spikes in ensembles of human tactile afferents code complex spatial fingertip events. *Nature Neurosci.*, 7:170–177, 2004.
- [17] E. Kandel, J. Schwartz, and T. Jessell. *Principles of Neural Science (third ed.)*. Elsevier/North-Holland, Amsterdam, London, New York, 1991.
- [18] D. Meunier, R. Lambiotte, and E. T. Bullmore. Modular and hierarchically modular organization of brain networks. *Front. Neurosci.*, 4:200, 2010.
- [19] M. Oram, D. Xiao, B. Dritschel, and K. Payne. The temporal resolution of neural codes: does response latency have a unique role? *Trans. R. Soc. Lond. B*, 357:987–1001, 2002.
- [20] T. Pereira, Baptista M. S., and J. Kurths. General framework for phase synchronization through localized sets. *Phys. Rev. E*, 75:026216, 2007.
- [21] T. Pereira, Baptista M. S., and J. Kurths. Phase and average period of chaotic oscillations. *Phys. Let. A*, 362:159–165, 2007.
- [22] D. H. Perkel and T. H. Bullock. Neural coding. *Neurosciences Research Symposium Summaries. The MIT Press*, 3:405–527, 1969.
- [23] Michael W Reimann, Max Nolte, Martina Scolamiero, Katharine Turner, Rodrigo Perin, Giuseppe Chindemi, Paweł Dłotko, Ran Levi, Kathryn Hess, and Henry Markram. Cliques of neurons bound into cavities provide a missing link between structure and function. *Frontiers in Computational Neuroscience*, 11:48, 2017.
- [24] E. Schneidman, M. J. Berry, R. Segev, and Bialek W. Weak pairwise correlations imply strongly correlated network states in a neural population. *Nature*, 440:1007–12, 2006.
- [25] M. N. Shadlen and W. T. Newsome. Noise, neural codes and cortical organization. *Current Opinion in Neurobiology*, 4(4):569–579, 1994.
- [26] C. E. Shannon. A mathematical theory of communication. *The Bell System Technical Journal*, 27:379, 1948.
- [27] O. Sporns. *Networks of the brain*. Cambridge MA: The MIT Press, 2011.
- [28] G. B. Stanley. Reading and writing the neural code. *Nature Neuroscience*, 16:259–263, 2013.
- [29] R. B. Stein, E. R. Gossen, and K. E. Jones. Neuronal variability: Noise or part of the signal? *Nat. Rev. Neurosci.*, 6(5):389–397, 2005.
- [30] S. Thorpe, F. Fize, and C. Marlot. Speed of processing in the human visual system. *Nature*, 381:520–522, 1996.
- [31] G. Zamora-López, C. S. Zhou, and J. Kurths. Cortical hubs form a module for multisensory integration on top of the hierarchy of cortical networks. *Front. Neuroinform.*, 4:1, 2010.